XLIII CILAMCE
21–25, November, 2022
FOZ DO IGUAÇU – PR – BRAZIL

# A coupled finite element-meshfree smoothed point interpolation method for phase-field modelling

Larissa Novelli[1], Samir S. Saliba[1], Lapo Gori[1], Roque L. S. Pitangueira[1]

[1]*Dept. of Structural Engineering, Federal University of Minas Gerais*
*Pres. Antonio Carlos, 6627, School of Engeneering - Building 1, Pampulha, Belo Horizonte/MG, Brazil*
*larissan@ufmg.br, samirsaliba@yahoo.com, lapo@dees.ufmg.br, roque@dees.ufmg.br*

**Abstract.** The present work investigates the coupling between the finite element method (FEM) and smoothed point interpolation methods (SPIM) for the solution of crack propagation problems. The region of the model where the crack propagates is previously discretised by the SPIM method and the rest of the domain is represented by the FEM. The phase-field model is adopted as a constitutive model to simulate the degradation of the material during the analysis. In this model, the crack is considered as a diffuse crack where a length scale parameter controls the size of the diffusive region and the phase field value indicates the integrity of the material. The computational implementations were performed in the INSANE (INteractive Structural ANalysis Environment) system, developed at the Department of Structural Engineering of the Federal University of Minas Gerais. Numerical simulations are performed using different smoothing domains and support nodes selection strategies. The results of simulations are compared with the standard finite element method in the complete domain.

**Keywords:** Smoothed Point Interpolation Methods (S-PIMs), FEM-SPIM coupling, Phase-field modelling

## 1 Introduction

The phase-field modelling was proposed by Francfort and Marigo [1] for propagation of complex cracks. In this model, the crack is represented as a diffuse entity where the phase-field variable represents the state of the material. There are different constitutive models based on the phase field model, for brittle fracture [1] and for quasi-brittle fracture [2].
To solve the equations of this method it is necessary to discretise the domain. Many works use the finite element method (FEM) [3, 4], but the meshfree methods can also be used. In a recent work, Novelli et al. [5] studies the use of meshfree Smoothed Point Interpolation Methods (SPIM) for the discretisation of phase-field modelling for brittle fracture. This work illustrated that the different SPIM strategies are able to correctly reproduce the contour plots of crack and that the load–displacement paths depend on the smoothed domain. However, these methods have a high preprocessing cost as a disadvantage.
In Saliba et al. [6], the coupled FEM-SPIM is discretised for the solution of damage models. In this strategy, the model is discretised with SPIM in the region of the growth of the damage and with FEM in the rest of the domain. In this article, the coupled FEM-SPIM for phase-field modelling is implemented. Simulations are performed using INSANE (Interactive Structural ANalisys Environment)[1] and problems of brittle fracture and quasi-brittle fracture are analysed.

## 2 Phase-field modelling

The phase-field modelling is based in the variational formulation of Griffith's, which considers an isotropic elastic body $\Omega$ with sharp crack $\Gamma$, with prescribed body forces $\boldsymbol{b}$ and surface forces $\boldsymbol{t}$, as shown in Fig. 1(a). The boundary is composed by $\partial\Omega = \partial\Omega_t \cup \partial\Omega_u$, where $\partial\Omega_t$ is the region where the loadings are applied, while $\partial\Omega_u$ is the region of prescribed displacements. In the phase field theory, the crack $\Gamma$ is modelled as a diffuse entity as illustrated in Fig. 1(b). The total energy functional of the body is given by:

[1]More information on the project can be found at https://www.insane.dees.ufmg.br/; the development code is freely available at the Git repository http://git.insane.dees.ufmg.br/insane/insane.git.

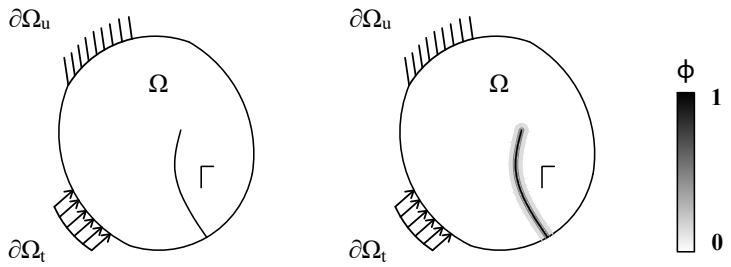


(a) (b)

Figure 1. Elastic body with a crack.

$$E_t = \int_\Omega \psi(\boldsymbol{\varepsilon}(\boldsymbol{u}), \phi) dV + \int_\Omega G_c \gamma(\phi, \nabla\phi) dV - \int_\Omega \boldsymbol{b} \cdot \boldsymbol{u} dV - \int_{\partial\Omega} \boldsymbol{t} \cdot \boldsymbol{u} dA. \tag{1}$$

where $G_c$ is the fracture energy.

The diffuse crack is represented in terms of a crack surface density function, given by the eq. 2. The variable $\phi$ describe the state of the material, being 0 for intact material and 1 for completely broken material and a length scale parameter $l_0$ defines the width of the diffuse region.

$$\delta_\phi \gamma = \frac{1}{c_0}[\frac{1}{l_0}\alpha'(\phi) - 2l_0\Delta\phi] \tag{2}$$

where $\alpha(\phi)$ is the geometric crack function and $c_0 := 4\int_0^1 \alpha^{\frac{1}{2}}(\hat{\phi})d\hat{\phi}$. The geometric crack function must be values between $\alpha(0) = 0$ e $\alpha(1) = 1$. Wu [2] suggest the general formulation for this function, given by:

$$\alpha(\phi) = \xi\phi + (1-\xi)\phi^2 \in [0,1] \; \forall\phi \in [0,1] \tag{3}$$

where $\xi \in [0,2]$. In this work, is adopted $\xi = 0$, resulting in $\alpha(\phi) = \phi^2$ and $\xi = 2$, resulting in $\alpha(\phi) = 2\phi - \phi^2$.

The dependence of the strain energy on the phase-field is represented in terms of a degradation function $g(\phi)$. To prevent crack growth under compression, the degradation function is usually applied only to the positive part of the strain energy:

$$\psi(\boldsymbol{\varepsilon}(\boldsymbol{u}), \phi) = g(\phi)\psi_0^+(\varepsilon) + \psi_0^-(\varepsilon) \tag{4}$$

In the literature there are different energy degradation functions. They must verify the values $g(0) = 1$ and $g(1) = 0$ for represent the intact material and the broken material, respectively.

In the model of Miehe et al. [7], the spectral decomposition of the strain tensor is used and the $g(\phi)$ is given by:

$$g(\phi) = (1-\phi)^2 + k \tag{5}$$

where $k$ is a small value used to prevent numerical singularities.

In the model of Wu [2], $g(\phi)$ is given by:

$$\frac{(1-\phi)^p}{(1-\phi)^p + Q(\phi)} \qquad Q(\phi) = a_1\phi + a_1a_2\phi^2 + a_1a_2a_3\phi^3 \tag{6}$$

where the parameters $a_1$, $a_2$, $a_3$, and $p$ can be related with material properties and the softening laws.

$$a_1 = \frac{2E_0G_f}{f_t^2} \cdot \frac{\xi}{C_0 l_0} \tag{7}$$

where $f_t$ is the material tension strength. The softening law frequently adopted for quasi-brittle failure is the Cornelissen softening curve. This law adopts: $p = 2$, $a_2 = 1.3868$ and $a_3 = 0.6567$.

To find the displacement ($u$) and the phase-field ($\phi$) it is necessary to minimise the total energy functional, imposing also the irreversibility ($\phi \leq 0$) and bounding ($\phi \in [0,1]$). This minimization result in a system with two equations, an related to displacements and other related do phase-field. To solved these equations are used the staggered solvers. Miehe et al. [7] proposed the use of the effective crack driving force as a historical variable (H) that represents the maximum tensile energy to guarantee the irreversibility, but this strategy can be used only with

$\xi = 0$ and $g(\phi)$= Eq. 5. This strategy was implemented in the INSANE by Leão et al. [3]. When other $\xi$ and $g(\phi)$ are used is adopted the bound-constrained solver. In this method is solved the constrained minimisation problem with the reduced space active set. This solver was implemented in the INSANE by Bayao et al. [4].

## 3 Coupling between the Finite Element Method (FEM) and Smoothed Point Interpolation Methods (SPIM)

To solve the phase-field problem the domain must be discretised. For this, one can use the finite element method or other strategies such as meshfree methods. Different from the FEM, in meshfree methods, the approximation functions are constructed, at each point of the domain, considering a set of nodes in the neighbourhood of the point of interest, called *support nodes*.

In this work, the coupling between FEM and meshfree methods is used to discretise de domain. This coupling between different methods is possible when the compatibility of the approximation in the transition zone is guaranteed. The meshfree method adopted is the SPIM proposed by Liu [8]. This method uses the Point Interpolation Method (PIM) for shape functions construction, where the approximation is an interpolation of the field variables values at each scattered node within a support domain. The radial point interpolation method with polynomial reproduction (RPIMp) [9] can also be used to construct this shape functions. The main advantage of this functions with respect to other meshfree shape functions is that they possess the Kronecker delta property. This property is very important in the case of coupling methods because the compatibility at the interface between the subdomains is automatically satisfied, and no additional techniques are needed. However possible discontinuities in the shape functions, may occur in the meshfree domain when switching from a support domain to another.

To deal with this issue, Liu and his co-authors [8] proposed the use of SPIM, where the derivatives of the shape functions is obtained by smoothed derivatives. In this case, the domain is divided into a set of smoothing domains, which are usually created using triangular background cells. Figure 2 presents the cell- and edge-based smoothed domains.

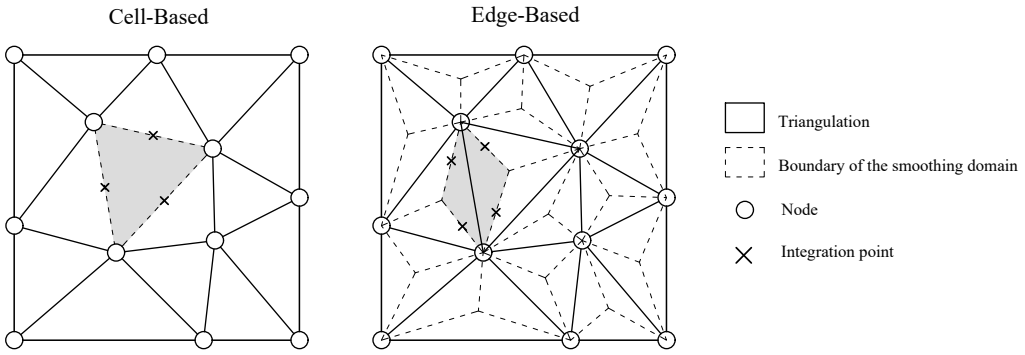


Figure 2. Illustration of the smoothing domains.

The same background cells used to build the smoothing domains can also be used to select the nodes of the support domain that will be used to build the shape functions. In this work are used T4-schemes for cell-based, and T3 and T6/3 for edge-based, as illustrated in Fig. 3.

## 4 Numerical simulations

This section illustrates the numerical results obtained by coupling FEM-SPIM to the phase-field modelling. Two examples present in the literature are analysed. For each problem, RPIMp shape functions were adopted for cell-based and edge-based. For comparison purposes, the results obtained with the FEM in complete domain were presented, performed using the same triangular meshes of the cells.

### 4.1 Tension test

The first example refers the tension test simulated by Miehe et al. [7]. This problem was performed using the crack shape function $\alpha = \phi^2$, the energetic degradation function $g(\phi) = (1-\phi)^2 + k$ and spectral decomposition of the strain tensor similar to adopted in Miehe et al. [7]. The model is illustrated in Fig. 4. The material was

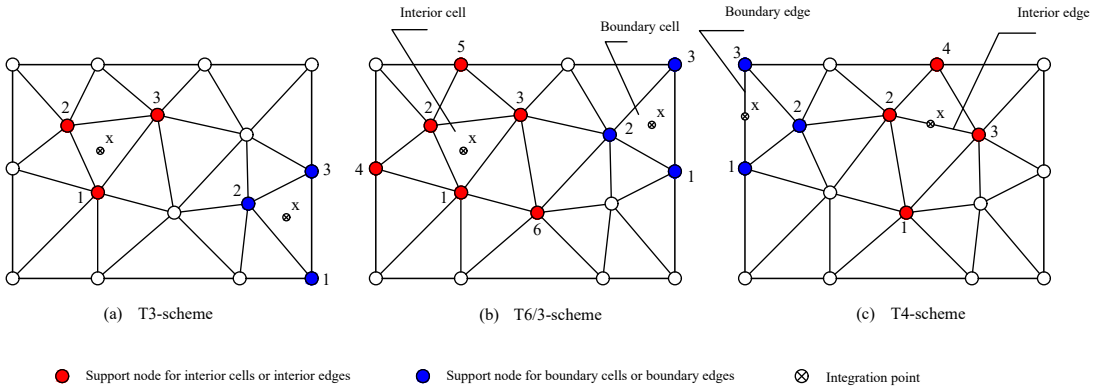


Figure 3. T-schemes for supporting nodes selection.

modelled considering a Young's modulus E = 210 kN/mm$^2$, Poisson's ratio $\nu = 0.3$, critical energy release rate $G_c$ = 0.0027 kN/mm and length scale parameter $l_0$ = 0.015 mm. The plane-strain state is adopted.

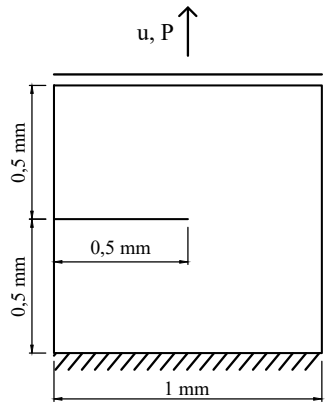


Figure 4. Tension test: Geometry, loading and boundary conditions.

The domain was discretised considering a nodal spacing of 0.0075 mm in the region where the phase-field propagation was expected. In this region is adopted the meshfree model. The coupled meshes are illustrated in Fig. 5 where the color blue represent the region of MEF and the color red represent the meshfree region. The Fig. 5 c) show a zoom in the region of edge-based smoothed domain.

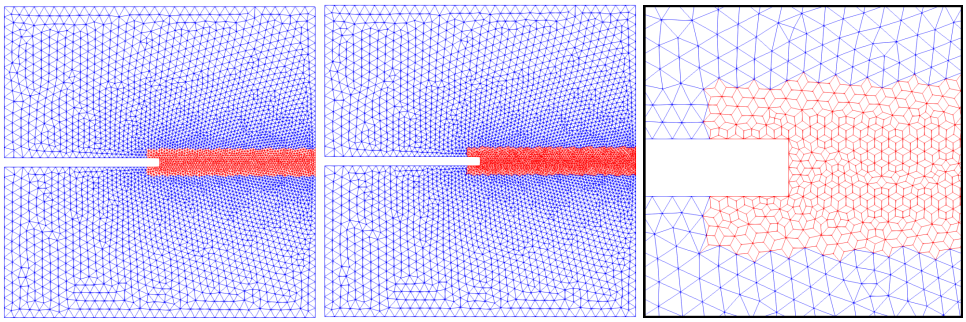

(a) FEM-Cell based (b) FEM-Edge based (c) FEM-Edge based Zoom

Figure 5. Coupled FEM-SPIM mesh of the tension test.

The nonlinear process was performed by the direct displacement control method, considering increments of $\Delta u = 1 \times 10^{-4}$ mm of the top edge in the vertical direction for all the steps. The load-displacement curves are shown in Fig. 6 together with the reference solution by Miehe et al. [7] and the FEM for the complete domain.

As it can be observed, the results are in good agreement with the ones obtained by Miehe et al. [7]. For all

strategies, the peak load was similar. It is possible to observe that the coupled FEM-Edge based with T6/3 scheme presented more points in the post-critical curve. This result is assigned to the number of nodes in the support domain.

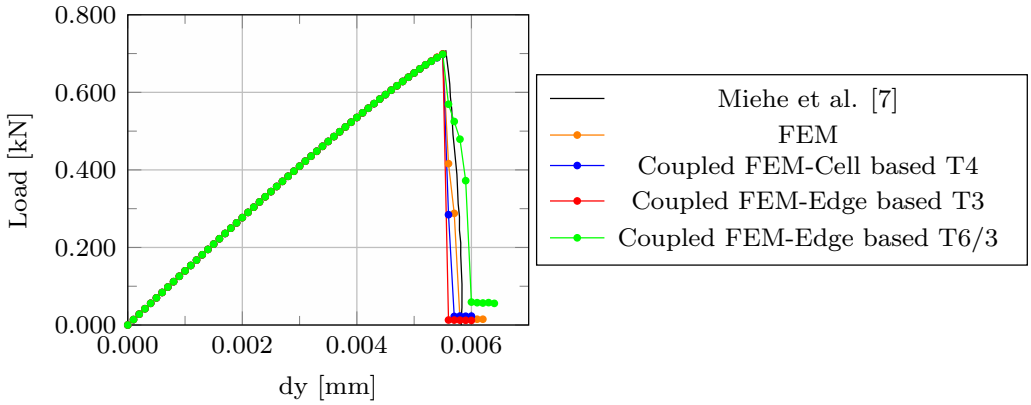


Figure 6. Load-displacement curve of the tension test.

Figure 7 presents the total number of iterations of each nonlinear process. These iterations correspond the ones named "global iterations", which represent the convergence of both the displacement and phase field equations in a staggered solver.

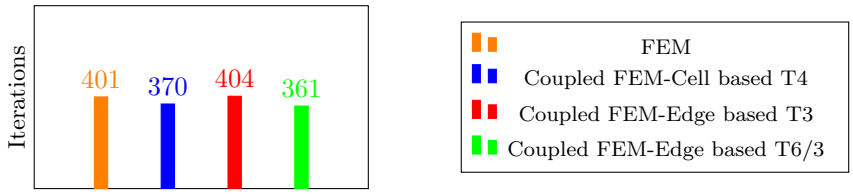


Figure 7. Total number of iterations of the analysis.

The contour plots of the nodal values of the phase-field for the coupled edge-based T6/3 schemes are illustrated in Fig. 8. It is possible observe that the evolution of the phase-field is similar to presented in Miehe et al. [7].

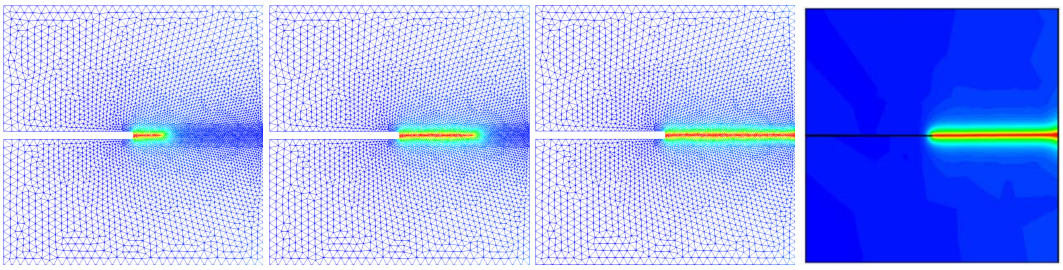


Figure 8. Phase-field contour plots for the tension test with coupled FEM-Edge based T6/3. Displacements of (a) $5.6 \times 10^{-3}$ mm, (b) $5.9 \times 10^{-3}$ mm, (c) $6.0 \times 10^{-3}$ mm and (d) Reference [7].

### 4.2 Bending test

The second example refers the test of four-point bending concrete notched beams reported in Hordijk [10] and illustrated in Fig. 9. The vertical force is $P = 0.5$ kN. This problem was simulated by Wu [11] using the crack shape function of the eq. 3 with $\xi = 2$ and the energetic degradation function of the eq. 6 with $p = 2$, $a_2 = 1.3868$ and $a_3 = 0.6567$. The material properties are: Young's modulus E = 38.0 kN/mm$^2$, Poisson's ratio $\nu = 0.2$, critical energy release rate $G_c = 1.25 \times 10^{-4}$ kN/mm, $f_t = 3 \times 10^{-3}$ kN/mm$^2$ and length scale parameter $l_0 = 5$ mm. The plane-stress state is adopted.

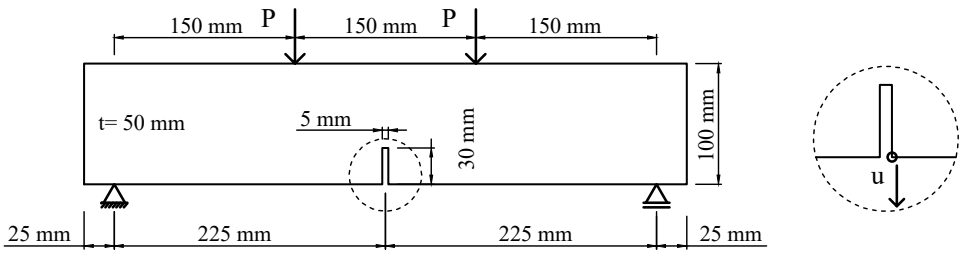


(a)

Figure 9. Bending test: Geometry, loading and boundary conditions.

The discretisations used in the analysis are shown in Fig. 10, where the color blue represent the MEF domain and the color red represent the meshfree domain. The refined region has nodal spacing of 1 mm.

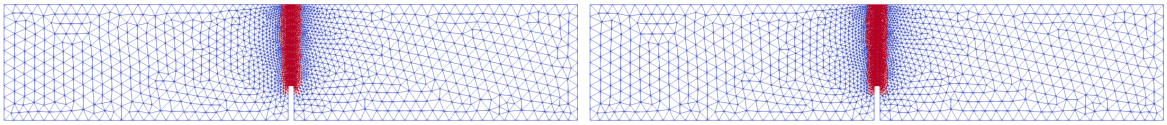

(a) FEM-Cell based (b) FEM-Edge based

Figure 10. Coupled FEM-SPIM mesh of the bending test.

The nonlinear process was performed by the direct displacement control method, considering increments of $\Delta u = -3.5 \times 10^{-3}$ mm of the vertical direction of the control node depicted in Fig. 9 for all the steps. The load-displacement curves are shown in Fig. 11 together with the experimental result by Hordijk [10], the numerical solution performed by Wu [11] and the complete domain with FEM. It can be observed that all the curves are in good agreement with the ones obtained by [10] and [11].

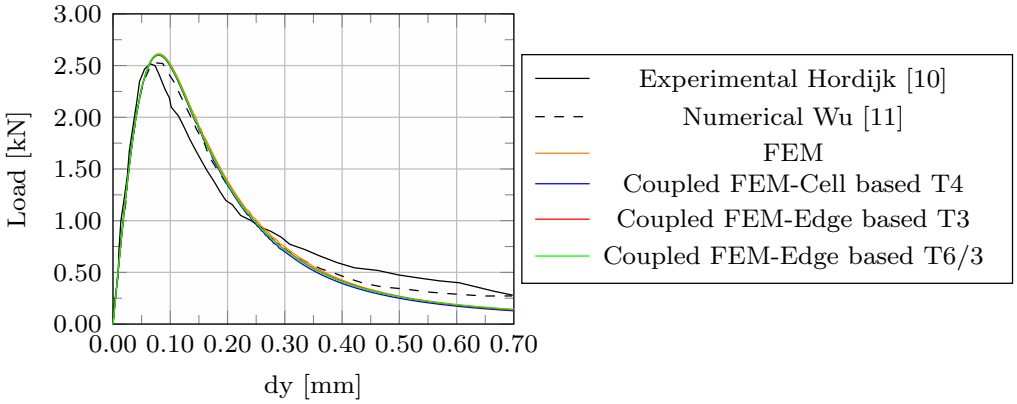


Figure 11. Load-displacement curve of the bending test.

The contour plots of the phase-field for the coupled cell-based T4 schemes are illustrated in Fig. 12. The phase-field evolution are according with the Wu [11].

## 5 Conclusions

This paper presented the use of the coupled FEM-SPIM for the discretisation of the phase-field modelling. Smoothing domains of the type cell and edge based and RPIMp shape functions with T3, T4 and T6/3 schemes for support nodes selection were used. Since to this shape functions posses the Kronecker delta property, this coupling can be doing directly.

Two numerical simulations were shown to study this strategy, the tension test and the bending test. The results were compared with the literature and with complete domain with FEM. The load-displacement curves obtained

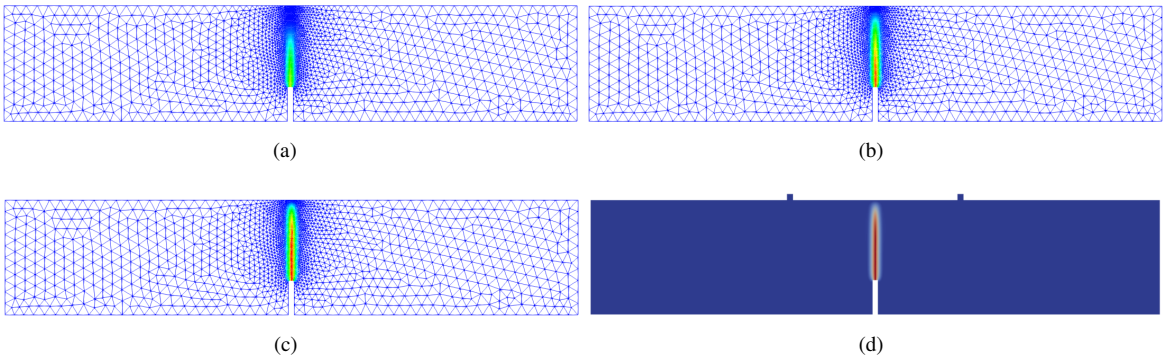


Figure 12. Phase-field contour plots for the bending test with coupled FEM-CS-RPIMp T4. Displacements of (a) 0.175 mm, (b) 0.35 mm, (c) 0.70 mm and (d) Reference [11].

in both test presented a good agreement with the results of the literature and FEM. Comparing the total number of iterations for the stress test, it is observed that the coupled FEM-Edge based on T6/3 presented a smaller number of iterations.
The contour plots for the phase-field were analysed too and the results were similar to those of the literature.

**Acknowledgements.** The authors gratefully acknowledge the support from the Brazilian research agencies CAPES (*Coordenação de Aperfeiçoamento de Pessoal de Nível Superior*), FAPEMIG (*Fundação de Amparo à Pesquisa do Estado de Minas Gerais*; Grant PPM-00747-18) and CNPq (Conselho Nacional de Desenvolvimento Científico e Tecnológico; Grant 316240/2021-4).

**Authorship statement.** The authors hereby confirm that they are the sole liable persons responsible for the authorship of this work, and that all material that has been herein included as part of the present paper is either the property (and authorship) of the authors, or has the permission of the owners to be included here.

## References

[1] G. A. Francfort and J. J. Marigo. Revisiting brittle fracture as an energy minimization problem. *J Mech Phys Solids*, vol. 46(8), pp. 1319–1342, 1998.
[2] J. Y. Wu. A unified phase field theory for the mechanics of damage and quasi-brittle failure. *Journal of the Mechanics and Physics of Solids*, vol. 103, pp. 72–99, 2017.
[3] H. Leão, R. L. S. Pitangueira, L. Gori, and S. S. Penna. Phase-field modelling of size effect on strength and structural brittleness. *Journal of the Brazilian Society of Mechanical Sciences and Engineering*, vol. 43, 2021.
[4] R. G. Bayao, H. M. Leão, M. M. Fortes, L. Gori, and R. L. S. Pitangueira. Implementation of a bound-constrained solver in phase-field modelling of fracture. In *Proceedings of the XLII Ibero-Latin-American Congress on Computational Methods in Engineering and III Pan-American Congress on Computational Mechanics*, 2021.
[5] L. Novelli, L. Gori, and R. L. S. Pitangueira. Phase-field modelling of brittle fracture with smoothed radial point interpolation methods. *Engineering Analysis with Boundary Elements*, vol. 138, pp. 219–234, 2022.
[6] S. S. Saliba, L. Gori, and R. L. S. Pitangueira. A coupled finite element-meshfree smoothed point interpolation method for nonlinear analysis. *Engineering Analysis with Boundary Elements*, vol. 128, pp. 1–18, 2021.
[7] C. Miehe, F. Welschinger, and M. Hofacker. Thermodynamically consistent phase-field models of fracture: Variational principles and multi-field fe implementations. *International Journal for Numerical Methods in Engineering*, vol. 83, pp. 1273–1311, 2010.
[8] G. Liu. *Meshfree Methods: Moving Beyond the Finite Element method*. CRC Press, New York, 2009.
[9] J. G. Wang and G. R. Liu. A point interpolation meshless method based on radial basis functions. *International Journal for Numerical Methods in Engineering*, vol. 54, pp. 1623–1648, 2002.
[10] D. Hordijk. *Local approach to fatigue of concrete*. PhD thesis, Delft University of Technology, Delft, The Netherlands, 1991.
[11] J. Y. Wu. A geometrically regularized gradient-damage model with energetic equivalence. *Computer Methods in Applied Mechanics and Engineering*, vol. 328, pp. 612–637, 2018.